Influence of neutral gas on Scrape-off layer tokamak plasma

N. Bisai and P. K. Kaw

Institute for Plasma Research, Bhat, Gandhinagar-382428, India

Corresponding Author: nirmal@ipr.res.in

Abstract:

Molecule density in Scrape-off Layer (SOL) of tokamak plasma is normally high. These molecules take part in many important reactions with the plasma and can modify plasma turbulence. A two-dimensional model has been derived for this purpose to study the plasma turbulence in the presence of the neutral gas. The growth rate obtained from these equations has been presented using linear theory. It is observed that the growth rate decreases with the increase of the molecular density and increases with the neutral gas ionization coefficient. The nonlinear equations have been solved numerically using two different simulations that are simulations using uniform and nonuniform electron temperature. The simulation results have been analyzed to identify role of neutral gas and electron temperature of the plasma. It is found that the neutral gas modifies plasma profiles, electric fields and also reduces the plasma fluctuation levels.

1   Introduction

Influence of neutral gas in Scrape-off layer (SOL) region is very complex and has become an intensive research area. Neutral gas in tokamak plasma originates either because of recycling from the walls or by an external gas puffing during gas puff related experiments. The neutral gas can be either molecular or atomic in form, but most measurements indicate that the molecular density is much higher than the atomic density [1]. These reactions are described in Appendix. It is well known that plasma in the SOL region is highly turbulent in nature mainly because of the presence of interchange modes [2, 3, 4, 5, 6]. The magnitude of these modes depends on the density/pressure gradient that can be modified by the presence of the neutral gas as the electron impact ionization of the gas can generate extra electron and ion that can modify the gradient. It is also known that the radial gradient of the electron temperature can contribute to the generation of radial electric fields that can control the plasma turbulence self-consistently. In the presence of the neutral gas the temperature and its gradient will be modified as the electrons lose energy by ionizing and various nonionizing collisions with the neutral gas. Therefore, studies of the plasma turbulence in the presence of neutral gas and electron temperature are important.

A number of authors have investigated interaction of the neutral gas with the SOL plasma. Reduction of two-dimensional (2D) interchange turbulence using mono-energetic neutral beams has been studied in Ref.[7]. Extensive studies on the divertor/SOL stability have been done in Refs.[8, 9]. Recently, reduction of plasma fluctuations and shift of plasma turbulence spectrum towards the low frequency side of the 2D interchange waves has been reported [10]. The fluid description for the atomic neutrals had been used in Ref.[10] as some small tokamak like Aditya showed substantial low energy electrons [11]. Most recently the SOL turbulence has been studied in the presence of the neutral gas molecules using nonuniform electron temperature [12]. Only few important aspects of the neutral gas on the plasma turbulence have been studied such as modification of various plasma gradients, and reduction of fluctuating levels. In this work, we have studied the plasma turbulence in more details. We have added another model of uniform electron temperature in the presence of the neutral gas to identify the role of the radial electric fields and molecular gases on the plasma turbulence. Here, the molecules have been considered at room temperature so that the mean free path (mfp) will be much less than the SOL thickness which allows to use the fluid theory for the molecules. It is to be noted that there are slow as well as fast atoms, but these are not considered here as the density of these atoms is much lower than the density of the molecules.

2 Model equations and Numerical parameters

Most relevant reactions in the SOL region of the plasma have been described in Appendix. Model equations (multispecies) have been derived based on these reactions that consist of electron continuity, H_2^+ continuity, current balance, electron energy, neutral momentum, and neutral continuity equations. These are shown in the following,

$$\frac{\partial n}{\partial t} + \vec{\nabla} \cdot (n\vec{v}) = \langle \sigma_{ion} v_e \rangle nN + S_n, \tag{1}$$

$$\frac{\partial n_2}{\partial t} + \vec{\nabla} \cdot (n_2 \vec{u}_2) = \langle \sigma_{ion} v_e \rangle nN - \left[\langle \sigma_{idis} v_e \rangle + \langle \sigma_{idisr} v_e \rangle \right] nn_2, \tag{2}$$

$$\vec{\nabla} \cdot \vec{J} = 0, \tag{3}$$

$$\frac{3}{2} n \left(\frac{\partial}{\partial t} + \vec{v} \cdot \vec{\nabla} \right) T_e + p_e \vec{\nabla} \cdot \vec{v} = -\vec{\nabla} \cdot q_e + nS_{Te}, \tag{4}$$

$$2NM \frac{\partial \vec{V}}{\partial t} = -\vec{\nabla} p_N - 2MNn \left[\langle \sigma_{ion} v_e \rangle \vec{V} + \langle \sigma_{cx} v_e \rangle (n_2/n)(\vec{V} - \vec{u}) + \langle \sigma_{mdis} v_e \rangle \vec{V} \right], \tag{5}$$

$$\frac{\partial N}{\partial t} + \vec{\nabla} \cdot \left(N\vec{V} \right) = -nN \left[\langle \sigma_{ion} v_e \rangle + (n_2/n) \langle \sigma_{cx} v_e \rangle + \langle \sigma_{mdis} v_e \rangle \right] + S_N. \tag{6}$$

These equations also require $n = n_1 + n_2$. n, n_1, n_2, and N represent density of electrons, H^+ ions, H_2^+ ions, and neutral gas molecules, respectively. The symbols $\vec{v}$, $\vec{u_1}$, and $\vec{u_2}$ are velocity of electrons, H_2^+, and H^+ ions. These can be written as $\vec{v}_\perp + \vec{v}_\parallel$, $\vec{u_1} = \vec{u}_{1\perp} + \vec{u}_{1\parallel} + \vec{u}_{1in}$, and $\vec{u_2} = \vec{u}_{2\perp} + \vec{u}_{2\parallel} + \vec{u}_{2in}$ where the lower symbols $\perp$ and $\parallel$ indicate perpendicular, and parallel velocity components. The $\perp$ component includes various drift velocities like $\vec{E} \times \vec{B}$ ($\vec{E} = -\vec{\nabla}\phi$ is electric field, ϕ is electrostatic potential), diamagnetic, and polarization drifts. The terms $\vec{u}_{1in}$ and $\vec{u}_{2in}$ indicate velocity in $\vec{E}$ direction due to collision with neutral gas; $\vec{u}_{in} = (\nu_{in}/\Omega_s)(\vec{E}/B)$ where ν_{in} indicates collision frequency of ions with the neutral gas. Velocity of the neutral gas molecules is represented by $\vec{V}$. The terms $\langle \sigma_{ion} v_e \rangle$, $\langle \sigma_{mdis} v_e \rangle$, $\langle \sigma_{idis} v_e \rangle$, and $\langle \sigma_{idisr} v_e \rangle$, indicate molecular ionization, molecular dissociation, H_2^+ ionic dissociation, and H_2^+ ionic dissociative recombination rate coefficients, respectively. These are function of the temperature T_e. The term $\langle \sigma_{cx} v_e \rangle$ indicates charge exchange rate coefficient between H_2^+ and H. Electron pressure and neutral pressure are represented by p_e and p_N, respectively. The mass of H_2^+ is two times of the mass of H^+, which is represented by $2M$. The total current density $\vec{J}$ can be written as $\vec{J} = e(n_1\vec{u_1} + n_2\vec{u_2} - n\vec{v})$, where e represents electronic charge. The parameters S_n, nS_{Te}, and S_N represent plasma, electron energy, and neutral gas sources, respectively. Equations.(1)-(5) can be written as in the following 2D form;

$$\frac{dn}{dt} - D\nabla_\perp^2 n + g\left(T_e\frac{\partial n}{\partial y} + n\frac{\partial T_e}{\partial y} - n\frac{\partial \phi}{\partial y}\right) = \xi_{ion}(T_e)nN - \sigma n\sqrt{T_e}e^{\Lambda-\phi/T_e} + S_n, \quad (7)$$

$$\frac{\partial}{\partial t}\left(n_2 - 2n_2\nabla_\perp^2\phi\right) + [\phi, n_2] - D_{n2}\nabla_\perp^2 n_2 - 2n_2[\phi, \nabla_\perp^2\phi] - gn_2\frac{\partial \phi}{\partial y} = \xi_{ion}(T_e)nN - \xi_{eff}^{n_2}nn_2, \quad (8)$$

$$\frac{\partial \nabla_\perp^2\phi}{\partial t} + [\phi, \nabla_\perp^2\phi] - \nu\nabla_\perp^4\phi + \frac{g}{n+2n_2}\left(T_e\frac{\partial n}{\partial y} + n\frac{\partial T_e}{\partial y}\right)$$
$$= \sigma\frac{n}{n+2n_2}\sqrt{T_e}\left(1 - e^{\Lambda-\phi/T_e}\right) - \sigma\left(1 - \frac{1}{\sqrt{2}}\right)\frac{n_2}{(n+2n_2)} - \nu_{in}\nabla_\perp^2\phi, \quad (9)$$

$$\frac{dT_e}{dt} - k_e\nabla_\perp^2 T_e + \frac{2}{3}g\left(\frac{7}{2}T_e\frac{\partial T_e}{\partial y} + \frac{T_e^2}{n}\frac{\partial n}{\partial y} - T_e\frac{\partial \phi}{\partial y}\right) = -\frac{2}{3}f_{loss}\xi_{eff}^{loss}NT_e$$
$$- \frac{2}{3}\sigma T_e^{3/2}\left(1.71e^{\Lambda-\phi/T_e} - 0.71\right) + S_{Te}, \quad (10)$$

$$\frac{\partial N}{\partial t} - \vec{\nabla}_\perp \cdot \left[D_n(n)\vec{\nabla}_\perp N\right] = -\xi_{ion}^N nN + S_N. \quad (11)$$

where, $df/dt = \partial f/\partial t + [\phi, f]$. Few steps of the above calculations are given in Ref.[10]. Equations-(7)-(11) are in normalized form. Detailed normalization and descriptions of other parameters have been described in Ref.[12]. The temperature dependence of the cross-section has been indicated for the molecular ionization coefficient $\xi_{ion}(T_e)$.

3 Numerical parameters

Typical ADITYA tokamak related parameters have been used to calculate input parameters needed for solving the model equations. These are, electron temperature $T_{e0} \sim 14.2$ eV, the plasma density $n_0 \sim 5 \times 10^{18}$ m^{-3}, major radius $R \sim 0.75$ m, and magnetic field $B \sim 0.8$ Tesla. These estimate $g = 6.3 \times 10^{-4}$ and $\sigma = 2 \times 10^{-4}$. T_e dependence of the ionization cross-section can be approximated using the expression $\xi_{ion}(T_e) = \xi_{ion}\sqrt{T_e}e^{-1/T_e}$, where T_e is normalized by T_{e0} and $\xi_{ion} = 2.2 \times 10^{-4}$. Other cross-section related parameters are $\xi_{eff}^{n2} = 6.5 \times 10^{-3}$, $\xi_{eff}^{loss} = 6.5 \times 10^{-4}$, $f_{loss} = 2$, and $\xi_{eff}^{N} = 6.5 \times 10^{-4}$. The diffusion/conduction loss related parameters are $D = D_{n2} = \nu = k_e = 0.01$ and $D_n = 0.6$.

4 Linear Growth Rates

We have linearized Eqs.(7)-(11) using expansion of $f(x, y, t) = \bar{f}(x, t) + f(x, y, t)$, where f can be any variable like n, n_2, etc., and $\bar{f}$ indicates equilibrium values of the variables. We can take $\bar{n}(x, t) = \bar{T}_e(x, t) = 1$. The equilibrium potential can be represented by $\bar{\phi}(x, y, t) = \Lambda \bar{T}_e(x, t)$. The magnitude of $\bar{N}$ can be estimated by balancing parallel loss terms in Eq.(7); $\bar{N} = \sigma/\xi_{ion}(T_e)$. The equilibrium value of molecular ion density $\bar{n}_2$ can be estimated from balancing source and sing terms of Eq.(8), which is $\bar{n}_2 = \xi_{ion}(T_e)/\xi_{eff}^{n2}$. All the fluctuating terms $\tilde{f}$ can be expressed by $\tilde{f} \sim e^{-i\omega t + ik_y y}$. Linearized forms of Eqs.(7)-(11) can give rise to dispersion relation. The relation has been solved to get the most unstable root with respect to k_y. Figure-1(a) indicates that the growth rate (γ) decreases with the increase of $\bar{N}$. This is an important result as it indicates that stabilization of interchange modes by the presence of the neutral gas. Therefore, one can anticipate the similar stabilization nonlinearly from the numerical simulations. It is expected that if ξ_{ion} is increased then it can generate more plasma therefore the plasma loss through the sheath will not be enough to maintain the same level of the plasma stability. Therefore, the plasma can be destabilized by the presence of high ξ_{ion}. Figure.1(b) indicates that γ increases with ξ_{ion}.

5 Numerical Simulation and results

The 2D Eqs.(7)-(11) have been solved numerically. The numerical code uses finite difference along x direction and Fourier transformation along y direction. Neumann boundary condition along x and periodic along y have been used. The simulation has been done in $L_x \times L_y$ region where $L_x = 196$ and $L_y = 196$, both L_x and L_y are normalized by ρ_s. Detailed description of the code can be found in Ref.[12]. Here, two different numerical simulations are done, these are WNG_UTE (With neutral Gas using Uniform T_e), and WNG (With Neutral Gas).

The neutral gas profiles obtained from the WNG_UTE and WNG have been shown in Fig.2(a). The gas density is maximum at $L_x = 196$ as the sources of the neutral gas are present at this location. It is to be noted that the gas density (t and y averages) obtained
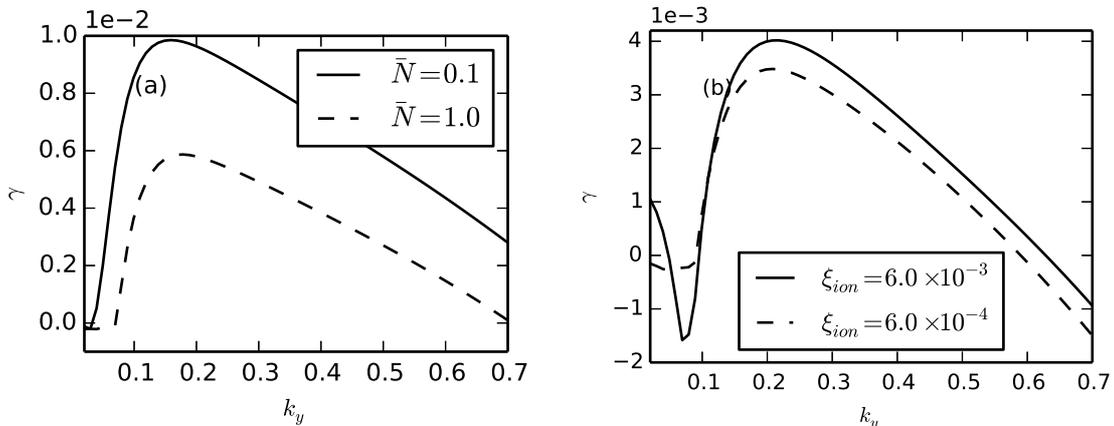
FIG. 1: (a) Growth rate decreases with neutral gas equilibrium density. (b) growth rate increases with ξ_{ion}.

from the WNG_UTE simulation is lower than from the WNG simulation even both the simulations have used the same gas source S_N. This has happened as the WNG_UTE uses uniform $T_{e0} = 14.2\text{eV}$ which is almost upper limit of the SOL temperature in the WNG. Therefore, the gas ionization is high in WNG_UTE. As $\xi_{ion}(T_e)$ increases with T_e, therefore, more gas ionization can be expected at lower values x where the energy source of S_{Te} is present. Also, plasma density is high at this location due to the presence of the particle sources that can increase the total numbers of molecular ionization for both the simulations. Therefore, strong absorption of N takes place at lower x.

Figure-2(b) shows plasma density obtained from both the simulation data. The density obtained from the WNG is higher than the WNG_UTE even less N ionizations takes place. This happens as plasma forms locally and the radial electric field (E_x) plays an important role for confinement of the plasma at this location. The field E_x generates from the radial gradient of T_e in WNG by $E_x \sim -\Lambda\partial T_e/\partial x$. E_x prevents the plasma to diffuse radially outward direction. In WNG_UTE simulation, the gas ionization takes place uniformly in the SOL and the radial electric field strength is negligibly small. Figure.2(b) indicates that the radial gradient of the density is higher in the WNG than the WNG_UTE, therefore, interchange turbulence can be stronger in WNG.

The molecular ion density (n_2) obtained from the WNG and WNG_UTE has been shown in Fig.3(a). It is interesting to observe that n_2 is maximum at $x = 0$ in the WNG simulation, but in WNG_UTE it is maximum at $x = L_x$. This can be explained from the right hand side (RHS) of Eq.(8). In WNG simulation, $\xi_{ion}(T_e)nN > \xi_{eff}^{n2}nn_2$ near $x = 0$, but in WNG_UTE the opposite is true near $x = L_x$. But the maximum value of $\langle n_2\rangle_{t,y}$ for the WNG and WNG_UTE can be estimated from $\langle n_2\rangle_{t,y} = \langle N\rangle_{t,y}\xi_{ion}(T_e)/\xi_{eff}^{n2}$. If we assume $T_e \sim 15\text{eV}$, then the ratio can be written as $\xi_{ion}(T_e)/\xi_{eff}^{n2} \sim 0.1$. For WNG_UTE, $\langle N\rangle_{t,y} \sim 0.12$ the molecular ion density can be $\langle n_2\rangle_{t,y} \sim 0.012$ that is shown in Fig.3(a) at $x = 0$. In WNG, the same estimation differs slightly mainly due to T_e dependence of the cross-section.
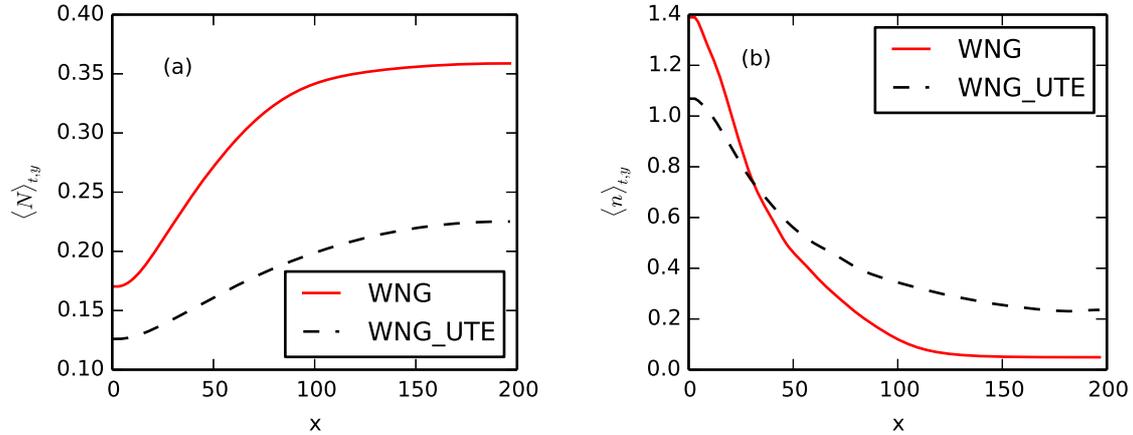
FIG. 2: (a)Neutral Gas profiles obtained from WNG and WNG_UTE simulations. $\langle N \rangle_{t,y}$ indicates time and poloidal averages. (b)Electron density profiles from the WNG and WNG_UTE simulations.

Fluctuation levels of n obtained from the two simulations have been compared where the fluctuation level of a physical parameter f is defined by $\tilde{\delta} f = \sqrt{\langle (f - \bar{f})^2 \rangle} / \langle f \rangle$; $\langle f \rangle$ indicates y and t averages of f. The fluctuation level of n is shown in Fig.3(b) where the level in the WNG is lower than the WNG_UTE. $\tilde{\delta} f$ for the other variables show the similar behavior. These indicate that N and T_e effectively reduce the fluctuation levels. Using spectrum analysis it is found that the high frequency part of the interchange turbulence has been most effected (reduced) by the neutral gas.

6   Summary and conclusions

The SOL plasma turbulence has been studied in the presence of the neutral gas molecules. The molecules are considered at room temperature so that the mfp is lower than the SOL thickness. Therefore, we have used fluid theory for the neutral gas. There is also atomic form of the neutral gas present in the SOL, but we do not include this as the density of these atoms is much lower than the molecules. In order to understand the influence of neutral gas linear and nonlinear studies have been done. The linear study indicates decrease of growth rate of the interchange modes in the presence of N. The growth rate increases with the increase of the ξ_{ion}. For the nonlinear studies, two different simulations have been done these are WNG and WNG_UTE. Electrons cool down in the presence of gas ionizations and other nonionizing collisions and hence T_e and N are coupled. The effect of T_e has been identified from comparing WNG and WNG_UTE results. Higher gradient of T_e has stabilizing influence. Plasma profiles, including profiles of n_2 have been calculated from the numerical data. Fluctuation levels of n and other variables are analyzed. It is found that the levels decrease considerably in the presence of N.
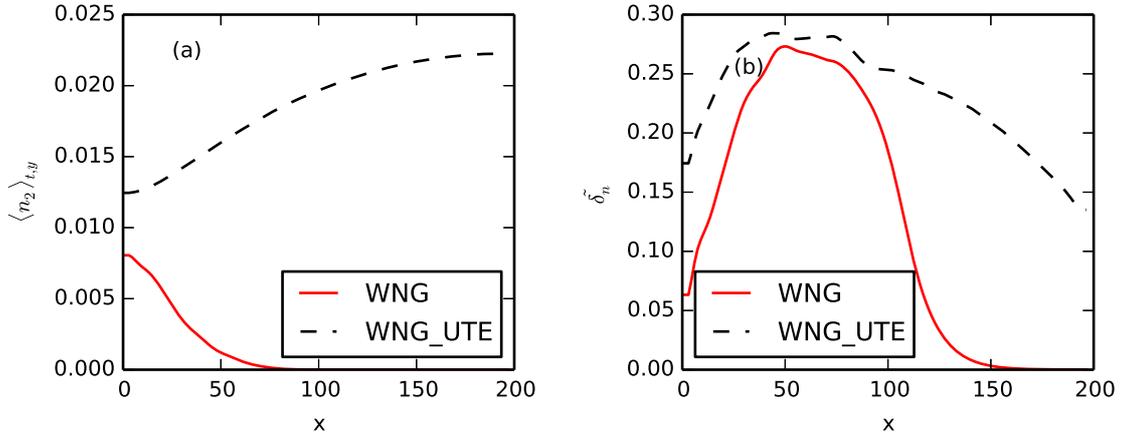
FIG. 3: (a)Radial profiles of H_2^+. (b)Reduction of $\tilde{\delta n}$ from two different simulations. Without N the level is higher than WNG and WNG_UTE [10].

Serial No.	Most relevant reactions in SOL
1	$H_2 + e \rightarrow 2H(n=1) + e$
2	$H_2 + e \rightarrow H_2^+ + 2e$
3	$H_2^+ + e \rightarrow H(n=1) + H^+ + e$
4	$H_2^+ + e \rightarrow H(1s) + H*(n>1)$
5	$H + e \rightarrow H^+ + 2e$

TABLE I: MOST RELEVANT ATOMIC AND MOLECULAR REACTIONS

Appendix: Important reactions

In SOL, many important atomic and molecular reactions are taking place in the presence of the ionizing electrons. The rate coefficients for these reactions (Table-I) are available in Refs. [1, 13, 14]. The dissociation of the molecular hydrogen into ground state atoms in the presence of $\sim$10-15eV electrons is given in reaction#1 that releases atoms with mean energy $\sim$3eV. At higher electron temperature, the hydrogen molecules preferentially ionized into hydrogen molecular ions (reaction#2) and further dissociated mainly through reaction#3 to produce atomic ions (H^+) and neutral atoms (H). The reaction#3 has a high rate coefficient. There is also dissociative recombination reaction (reaction#4) that a has high reaction rate coefficient specifically at $1 < T_e < 15$eV. Below 5eV the charge exchange of hydrogen molecules with protons dominates. There are other reaction channels (not shown in Table-I) also that can produce higher excited states of the atoms [1]. Some reactions can also produce slow neutral atoms with sub-eV and fast neutrals with energy greater than 3eV.

References

[1] CALL, E., et al., "Spatially resolved H_α-emission simulation with EIRENE in TJ-II to study hydrogen atomic and molecular physics in low density, high temperature fusion edge plasmas", Nucl. Fusion **48** (2008) 095005.

[2] SARAZIN, Y., GHENDRIH, P. H.,"Intermittent particle transport in two-dimensional edge turbulence", Phys. Plasmas **5** (1998) 4214.

[3] BISAI, NIRMAL., et al., "Simulation of plasma transport by coherent structures in scrape-off-layer tokamak plasmas", Phys. Plasmas **11** (2004) 4018.

[4] BISAI, N., et al., "Scrape-off layer tokamak plasma turbulence",Phys. Plasmas, **19** (2012) 052509.

[5] JHA, R., et al., "Intermitency in tokamak edge turbulence",Phys. Rev. Lett., **69** (1992) 1375.

[6] ZWEBEN, S. J., et al., "Edge turbulence imaging in the Alcator C-Mod tokamak", Phys. Plasmas **9** (2002) 1981

[7] MARANDET, Y., et al., "Influence of neutral particles on scrape-off layer turbulence with application to the interpretation of fast camera data", J. Nucl. Mater. **438** (2013) S518.

[8] D'IPPOLITO, D. A., and Myra, J. R., "Effect of neutrals on scrape-off layer and divertor stability in tokamaks", Phys. Plasmas, **6** (1999) 519.

[9] BEKHEIT, AMR-HASHEIM., "Simulation of Radial Variation of Neutral Atoms on Edge Plasma of Small Size Divertor Tokamak", Journal of Modern Physics, **3** (2012) 145.

[10] Bisai, N., et al., "Role of neutral gas in scrape-off layer tokamak plasma", Phys. Plasmas **22** (2015) 022517.

[11] FIELDING, S. J., et al., "Atom energy distributions from H_α lineshape measurements during gas puff experiments in DITE", J. Nucl. Mater., **162-164** (1989) 482–488.

[12] BISAI, N., Kaw, P. K., "Role of neutral gas in Scrape-off Layer of tokamak plasma in the presence of finite electron temperature and its gradient", Accepted for publication.

[13] JANEV, R. K., et al., "Elementary Processes in Hydrogen-Helium Plasma", Springer, Berlin, 1987.

[14] Janev, R. K., et al., "Atomic and molecular database for fusion plasma edge studies", Nucl. Fusion **29** (1989) 109.